arXiv:1512.06693v3 [math.ST] 13 Jul 2016

Towards optimal Takacs–Fiksel estimation

Jean-François Coeurjolly[1], Yongtao Guan[2], Mahdieh Khanmohammadi[3,4] and Rasmus Waagepetersen[5]

[1]Laboratory Jean Kuntzmann, Univ. Grenoble Alpes, France, Jean-Francois.Coeurjolly@univ-grenoble-alpes.fr
[2]Department of Management Science, University of Miami, USA, yguan@bus.miami.edu
[3]Department of Computer Science, University of Copenhagen, Denmark
[4]Department of Electrical Engineering and Computer Science, University of Stavanger, Norway, mh.khanmohammadi@gmail.com
[5]Department of Mathematical Sciences, Aalborg University, Denmark, rw@math.aau.dk

July 14, 2016

Abstract

The Takacs–Fiksel method is a general approach to estimate the parameters of a spatial Gibbs point process. This method embraces standard procedures such as the pseudolikelihood and is defined via weight functions. In this paper we propose a general procedure to find weight functions which reduce the Godambe information and thus outperform pseudolikelihood in certain situations. The new procedure is applied to a standard dataset and to a recent neuroscience replicated point pattern dataset. Finally, the performance of the new procedure is investigated in a simulation study.

Keywords: Gibbs point processes; Godambe information; optimal estimation; pseudolikelihood; spatial point processes.

1 Introduction

Spatial Gibbs point processes are important models for spatial dependence in point patterns (van Lieshout, 2000) with a broad range of applications (e.g. Stoyan and Penttinen, 2000; Illian *et al.*, 2008). Such processes are specified by a density with respect to a Poisson point process or, equivalently, by the Papangelou conditional intensity. When the density or Papangelou conditional intensity has a parametric form, popular options for parameter estimation include maximum likelihood (e.g. Ogata and Tanemura, 1984; Penttinen, 1984; Geyer, 1999; Møller and Waagepetersen, 2004), maximum pseudolikelihood (e.g. Besag, 1977; Jensen and Møller, 1991; Goulard *et al.*, 1996; Baddeley and Turner, 2000; Billiot *et al.*, 2008), maximum logistic regression likelihood (Baddeley *et al.*, 2014) and Takacs-Fiksel estimation (e.g. Fiksel, 1984; Takacs, 1986; Tomppo, 1986; Coeurjolly *et al.*, 2012).

Maximum likelihood estimation for a Gibbs point process requires computationally intensive estimation of an unknown normalizing constant in the density function. This explains why alternative estimation methods have been studied. Takacs-Fiksel estimation is an estimating function method based on the general Georgii-Nguyen-Zessin integral equation involving the Papangelou conditional intensity and a user-specified weight function. A particular choice of the weight function recovers the score of the pseudolikelihood. Pseudolikelihood estimation has an intuitively appealing motivation and is by far the most popular estimation method in practical applications of Gibbs point processes with a user-friendly implementation in the `spatstat` package (Baddeley and Turner, 2005). Logistic regression likelihood estimation for Gibbs point processes was recently introduced to eliminate a bias problem coming from the Berman-Turner approximation of the pseudolikelihood (Berman and Turner, 1992; Baddeley and Turner, 2000). The logistic regression can be viewed as a computationally efficient approximation of the pseudolikelihood. Hence in the following, we may not differentiate between the pseudolikelihood and the logistic regression methods.

There are infinitely many weight functions that can be used to obtain Takacs-Fiksel estimates and usually weight functions are chosen by ad hoc reasoning paying attention to ease of implementation or to handle patterns which are sampled in situ, like in Tomppo (1986). In the small scale simulation study in Coeurjolly *et al.* (2012), pseudolikelihood and Takacs-Fiksel methods are compared for the Strauss model. The weight functions used for the Takacs-Fiksel method resulted in explicit expressions for the parameter estimates (no optimization required). In this simulation study, smallest standard errors were obtained with the pseudolikelihood method. Based on a larger simulation study, Diggle *et al.* (1994) concluded that pseudolikelihood provided reasonable and robust estimates for any point process model and boundary condition considered although significant bias was observed in cases of point processes models with strong interaction. For the Takacs-Fiksel method, Diggle *et al.* (1994) used weight functions leading to an estimation procedure similar to minimum contrast estimation using the empirical K-function, see e.g. Waagepetersen and Guan (2009). The authors noted that this type of Takacs-Fiksel estimation gave poor results relative to pseudolikelihood, in particular for point process models with weak interaction. Diggle *et al.* (1994) concluded that the bias was small for both Takacs-Fiksel and pseudolikelihood in case of small-to-medium strength of interaction. Based on the existing literature it is not clear whether pseudolikelihood is an optimal Takacs-Fiksel method in terms of minimizing estimation variance and it is interesting to investigate whether and when the Takacs-Fiksel method can outperform pseudolikelihood.

In this paper our aim is to develop a systematic approach to construct a weight function that can lead to more efficient estimation than existing methods. Our approach is motivated by the one considered in Guan *et al.* (2015) who considered estimation of the intensity function of a spatial point process and identified the optimal estimating function within a class of estimating functions based on the Campbell formula (e.g. Møller and Waagepetersen, 2004). Their optimal estimating function was derived from a sufficient condition equating the sensitivity matrix for the optimal estimating function and the covariance between the optimal estimating

function and an arbitrary estimating function.

Extending the ideas in Guan *et al.* (2015) to Gibbs point processes is not straightforward. One problem is that covariances of Takacs-Fiksel estimating functions are not available in closed forms (see Section 2.4 for more details). For this reason our new weight function only approximately satisfies the aforementioned sufficient condition. Nevertheless, we show in a simulation study that the new weight function may yield better estimation accuracy and is closer to fulfilling the sufficient condition than pseudolikelihood. Another issue is that the practical implementation of the new method is more computationally demanding than the pseudolikelihood, especially for point patterns of high cardinality.

The rest of the paper is organized as follows. Section 2 gives background on Gibbs point processes and Takacs-Fiksel estimation and presents our new methodology. In Section 3 we apply the methodology to the Spanish towns dataset as well as a recent replicated point pattern dataset from neuroscience. Motivated by these two examples, Section 4 presents a simulation study. Details of implementation are given in Appendix A.

2 Background and methodology

2.1 Gibbs point processes

A point process $\mathbf{X}$ on $\mathbb{R}^d$ is a locally finite random subset of $\mathbb{R}^d$, meaning that $\mathbf{X} \cap B$ is finite for every bounded $B \subset \mathbb{R}^d$. In this paper we assume that $\mathbf{X}$ is confined to and observed on a bounded region $W \subset \mathbb{R}^d$ so that $\mathbf{X}$ becomes a finite point process taking values in Ω, the set of finite point configurations in W.

The distribution of $\mathbf{X}$ is assumed to be specified by a parametric density $f(\cdot;\theta) : \Omega \to [0,\infty)$ with respect to the Poisson process of unit intensity. The density is of the form

$$f(\mathbf{y};\theta) \propto H(\mathbf{y})e^{V(\mathbf{y};\theta)} \tag{2.1}$$

where $\theta \in \Theta \subseteq \mathbb{R}^p$ is a p-dimensional parameter vector, $H : \Omega \to [0,\infty)$ serves as a baseline or reference factor, and $V : \Omega \to \mathbb{R}$ is often called the potential. For the Strauss model, for example, $H(\mathbf{y}) = 1$, $\theta = (\theta_1, \theta_2)$ and

$$V(\mathbf{y};\theta) = \theta_1 n(\mathbf{y}) + \theta_2 s_R(\mathbf{y})$$

where $n(\mathbf{y})$ is the cardinality of $\mathbf{y}$ and for $R > 0$, $s_R(\mathbf{y})$ is the number of subsets $\{u, v\}$, $u, v \in \mathbf{y}$, of pairs of R-close neighbours in $\mathbf{y}$. Thus values of $\theta_2 < 0$ promote point configurations with few R-close neighbours. The Strauss hard core model is the modification of the Strauss model where $H(\mathbf{y})$ is one if all interpoint distances are greater than some hard core distance $0 \leq \delta < R$ and zero otherwise. Thus for the Strauss hard core model, all points must be separated by a distance greater than δ.

Assuming that H is hereditary, i.e. $H(\mathbf{y} \cup u) > 0$ implies $H(\mathbf{y}) > 0$ for any $u \in W$ and $\mathbf{y} \in \Omega$, the Papangelou conditional intensity of $\mathbf{X}$ exists and is defined by

$$\lambda(u, \mathbf{y};\theta) = \frac{f(\mathbf{y} \cup u;\theta)}{f(\mathbf{y};\theta)} = H(u, \mathbf{y})e^{V(u,\mathbf{y};\theta)}$$

where $H(u, \mathbf{y}) = \mathbf{1}\{H(\mathbf{y}) > 0\}H(\mathbf{y} \cup u)/H(\mathbf{y})$ and $V(u, \mathbf{y}; \theta) = V(\mathbf{y} \cup u; \theta) - V(\mathbf{y}; \theta)$. For the Strauss model, $H(u, \mathbf{y}) = 1$ and $V(u, \mathbf{y}; \theta) = \theta_1 + \theta_2 s_R(u, \mathbf{y})$ where $s_R(u, \mathbf{y})$ is the number of points in $\mathbf{y}$ with distance to u less than R. For the Strauss hard core model, $H(u, \mathbf{y})$ is one if all the points of $\mathbf{y} \cup u$ are separated by distances greater than δ and zero otherwise. In this paper we assume finite range, i.e. for some $0 < R < \infty$ and for any $u \in W$ and $\mathbf{y} \in \Omega$

$$\lambda(u, \mathbf{y}; \theta) = \lambda\{u, \mathbf{y} \cap B(u, R); \theta\} \tag{2.2}$$

where $B(u, R)$ is the ball with center u and radius R. Thus the conditional intensity of a point u given $\mathbf{y}$ only depends on the R-close neighbours in $\mathbf{y}$. This is obviously satisfied for the Strauss and Strauss hard core models. Intuitively, $\lambda(u, \mathbf{x}; \theta)\,\mathrm{d}u$ is the conditional probability that a point of $\mathbf{X}$ occurs in a small neighbourhood B_u of volume $\mathrm{d}u$ around the location u, given $\mathbf{X}$ outside B_u is equal to $\mathbf{x}$; see Georgii (1976) for a general presentation and Coeurjolly *et al.* (2015) for links with Palm distributions.

Note that λ and f are in one-to-one correspondence. Hence the distribution of $\mathbf{X}$ can equivalently be specified in terms of the Papangelou conditional intensity. Gibbs point processes can also be characterized through the Georgii-Nguyen-Zessin formula (see Georgii, 1976; Nguyen and Zessin, 1979), which states that for any $h : W \times \Omega \to \mathbb{R}$ (such that the following expectations are finite)

$$\mathrm{E} \sum_{u \in \mathbf{X}} h(u, \mathbf{X} \setminus u) = \mathrm{E} \int_W h(u, \mathbf{X}) \lambda(u, \mathbf{X}; \theta)\,\mathrm{d}u. \tag{2.3}$$

Conditions ensuring the existence of Gibbs point processes constitute a full research topic (see e.g. Dereudre *et al.*, 2012, and the references therein). In case of a finite Gibbs point process existence is equivalent to that the right hand side of (2.1) can be normalized to be a probability density. We here just note that the Strauss model exists whenever $\theta_1 \in \mathbb{R}$ and $\theta_2 \leq 0$ while the Strauss hard core model exists for all $\theta_1, \theta_2 \in \mathbb{R}$ when $\delta > 0$. Other examples of point process models can be found in Møller and Waagepetersen (2004); see also Section 3.2 for an example of an inhomogeneous model.

2.2 Takacs-Fiksel estimation

Let $h = (h_1, \ldots, h_q)^\top$ where $h_i : W \times \Omega \to \mathbb{R}$, $i = 1, \ldots, q$ are real functions parameterized by θ where q is greater than or equal to the dimension p of θ. Takacs-Fiksel estimation (Fiksel, 1984; Takacs, 1986) is based on the Georgii-Nguyen-Zessin formula (2.3) which implies that

$$\mathrm{E} \sum_{u \in \mathbf{X}} h_i(u, \mathbf{X} \setminus u; \theta) - \mathrm{E} \int_W h_i(u, \mathbf{X}; \theta) \lambda(u, \mathbf{X}; \theta)\,\mathrm{d}u = 0, \quad i = 1, \ldots, q. \tag{2.4}$$

In the original formulation of Takacs-Fiksel estimation, an estimate of θ was obtained by minimizing the sum of squares

$$\sum_{i=1}^{q} \left\{ \sum_{u \in \mathbf{X}} h_i(u, \mathbf{X} \setminus u; \theta) - \int_W h_i(u, \mathbf{X}; \theta) \lambda(u, \mathbf{X}; \theta)\,\mathrm{d}u \right\}^2.$$

Considering the case $p = q$, a related approach is to define a p-dimensional estimating function e_h by

$$e_h(\theta) = \sum_{u \in \mathbf{X}} h(u, \mathbf{X} \setminus u; \theta) - \int_W h(u, \mathbf{X}; \theta) \lambda(u, \mathbf{X}; \theta) \, \mathrm{d}u. \tag{2.5}$$

In the point process literature, the term Takacs-Fiksel estimate is also used for an estimate obtained by solving the estimating equation $e_h(\theta) = 0$ with respect to θ (see e.g. van Lieshout, 2000; Baddeley *et al.*, 2015)). This is the type of Takacs-Fiksel estimation considered in this paper. By (2.4) the function $e_h(\theta)$ is unbiased, i.e., $\mathrm{E}\, e_h(\theta) = 0$. The asymptotic properties of the Takacs-Fiksel estimate for a general weight function h have been established by Coeurjolly *et al.* (2012) including a derivation of the asymptotic covariance matrix.

With the weight function $h(u, \mathbf{y}; \theta) = \mathrm{d} \log \lambda(u, \mathbf{y}; \theta) / \mathrm{d}\theta$, (2.5) is the score function for the log pseudolikelihood function. The corresponding estimate can be obtained using standard statistical software and its statistical properties have been deeply studied in the literature (e.g. Jensen and Møller, 1991; Mase, 1999; Jensen and Künsch, 1994; Billiot *et al.*, 2008; Baddeley *et al.*, 2014). However, the pseudolikelihood score has not been shown to be optimal within the class of Takacs-Fiksel estimating functions. In the following section our aim is to construct a competitor to the pseudolikelihood in terms of statistical efficiency.

2.3 Towards optimality

We begin this section by reviewing key quantities related to estimating functions. We refer to Heyde (1997) or Guan *et al.* (2015, Section 2.3) for further details. For an estimating function e_h, the sensitivity matrix S_h is defined as $S_h = -\mathrm{E}\left\{\frac{\mathrm{d}}{\mathrm{d}\theta^\top} e_h(\theta)\right\}$ and the covariance matrix of the estimating function is $\Sigma_h = \mathrm{Var}\{e_h(\theta)\}$. From these the Godambe information matrix is obtained as

$$G_h = S_h^\top \Sigma_h^{-1} S_h.$$

In applications of estimating functions, the inverse Godambe matrix provides the approximate covariance matrix of the associated parameter estimate. An estimating function e_ϕ is said to be Godambe optimal in a class of estimating functions e_h indexed by a set C of functions h, if the difference $G_\phi - G_h$ is non-negative definite for all $h \in C$. Following Guan *et al.* (2015), a sufficient condition for e_ϕ to be optimal is that for every estimating function e_h, $h \in C$,

$$\mathrm{Cov}\{e_h(\theta), e_\phi(\theta)\} = S_h. \tag{2.6}$$

In the context of Takacs-Fiksel estimating functions (2.5),

$$\begin{aligned}\frac{\mathrm{d}}{\mathrm{d}\theta^\top} e_h(\theta) = &\sum_{u \in \mathbf{X}} \frac{\mathrm{d}}{\mathrm{d}\theta^\top} h(u, \mathbf{X} \setminus u; \theta) - \int_W \left\{ \frac{\mathrm{d}}{\mathrm{d}\theta^\top} h(u, \mathbf{X}; \theta) \right\} \lambda(u, \mathbf{X}; \theta) \, \mathrm{d}u \\ &- \int_W h(u, \mathbf{X}; \theta) \frac{\mathrm{d}}{\mathrm{d}\theta^\top} \lambda(u, \mathbf{X}; \theta) \, \mathrm{d}u.\end{aligned}$$

So by the Georgii-Nguyen-Zessin formula (2.3),

$$S_h = \mathrm{E} \int_W h(u, \mathbf{X}; \theta) \frac{\mathrm{d}}{\mathrm{d}\theta^\top} \lambda(u, \mathbf{X}; \theta) \, \mathrm{d}u. \tag{2.7}$$

The definition of the estimating function e_h actually corresponds to the concept of innovations for spatial point processes (Baddeley *et al.*, 2005). Coeurjolly and Rubak (2013) investigated the problem of estimating the covariance between two innovations which, here, corresponds to the covariance between two estimating functions. Assuming the right hand side below is finite, Coeurjolly and Rubak (2013, Lemma 3.1) established that

$$\begin{aligned}\mathrm{Cov}\{e_h(\theta), e_g(\theta)\} = \mathrm{E} \Big[& \int_W h(u, \mathbf{X}; \theta) g(u, \mathbf{X}; \theta)^\top \lambda(u, \mathbf{X}; \theta) \, \mathrm{d}u \\ & + \int_W \int_W h(u, \mathbf{X}; \theta) g(v, \mathbf{X}; \theta)^\top \left\{ \lambda(u, \mathbf{X}; \theta) \lambda(v, \mathbf{X}; \theta) - \lambda(\{u, v\}, \mathbf{X}; \theta) \right\} \mathrm{d}u \, \mathrm{d}v \\ & + \int_W \int_W \Delta_v h(u, \mathbf{X}; \theta) \Delta_u g(v, \mathbf{X}; \theta)^\top \lambda(\{u, v\}, \mathbf{X}; \theta) \, \mathrm{d}u \, \mathrm{d}v \Big]\end{aligned} \tag{2.8}$$

where for any $u, v \in W$ and any $\mathbf{y} \in \Omega$, the second order Papangelou conditional intensity $\lambda(\{u, v\}, \mathbf{y}; \theta)$ and the difference operator $\Delta_u h(v, \mathbf{y}; \theta)$ are given by

$$\begin{aligned}\lambda(\{u, v\}, \mathbf{y}; \theta) &= \lambda(u, \mathbf{y}) \lambda(v, \mathbf{y} \cup u; \theta) = \lambda(v, \mathbf{y}; \theta) \lambda(u, \mathbf{y} \cup v; \theta) \\ \Delta_u h(v, \mathbf{y}; \theta) &= h(v, \mathbf{y} \cup u; \theta) - h(v, \mathbf{y}; \theta).\end{aligned}$$

Returning to the condition (2.6), we introduce for any $\mathbf{y} \in \Omega$ the operator $T_{\mathbf{y}}$ acting on $\mathbb{R}^p$ valued functions g,

$$T_{\mathbf{y}} g(u) = \int_W g(v) t(u, v, \mathbf{y}; \theta) \, \mathrm{d}v, \tag{2.9}$$

where

$$t(u, v, \mathbf{y}; \theta) = \lambda(v, \mathbf{y}; \theta) \left\{ 1 - \frac{\lambda(v, \mathbf{y} \cup u; \theta)}{\lambda(v, \mathbf{y}; \theta)} \right\}. \tag{2.10}$$

The finite range property of the Papangelou conditional intensity implies that for any $v \notin B(u, R)$, $t(u, v, \mathbf{y}; \theta) = 0$. So the domain of integration in (2.9) is actually just $W \cap B(u, R)$. From (2.7)-(2.8), (2.6) is equivalent to $\mathrm{E}(A) + \mathrm{E}(B) = 0$ where

$$A = \int_W h(u, \mathbf{X}; \theta) \lambda(u, \mathbf{X}; \theta) \left\{ \phi(u, \mathbf{X}; \theta) - \frac{\lambda^{(1)}(u, \mathbf{X}; \theta)}{\lambda(u, \mathbf{X}; \theta)} + T_{\mathbf{X}} \phi(u, \mathbf{X}; \theta) \right\}^\top \mathrm{d}u \tag{2.11}$$

$$B = \int_W \int_W \Delta_v h(u, \mathbf{X}; \theta) \Delta_u \phi(v, \mathbf{X}; \theta)^\top \lambda(\{u, v\}, \mathbf{X}; \theta) \, \mathrm{d}u \, \mathrm{d}v \tag{2.12}$$

and $\lambda^{(1)}(u, \mathbf{X}; \theta) = \mathrm{d}\lambda(u, \mathbf{X}; \theta) / \mathrm{d}\theta$.

The expectation $\mathrm{E}(B)$ is very difficult to evaluate. Moreover, in the context of asymptotic covariance matrix estimation for the pseudolikelihood, Coeurjolly and Rubak (2013) remarked that the contribution of the term (2.12) to the covariance

$\mathrm{Cov}\{e_h(\theta), e_\phi(\theta)\}$ was negligible. In the following we will neglect the term (2.12) and call 'semi-optimal' a function $\phi : W \times \Omega \to \mathbb{R}^p$ (parameterized by θ) such that for any $h : W \times \Omega \to \mathbb{R}^p$, $\mathrm{E}(A) = 0$. We discuss this choice in more detail in Section 2.4. Considering (2.11), ϕ is semi-optimal if for any $\mathbf{y} \in \Omega$, $\phi(\cdot, \mathbf{y}; \theta)$ is the solution to the Fredholm integral equation (e.g. chapter 3 in Hackbusch, 1995)

$$\phi(\cdot, \mathbf{y}; \theta) + T_{\mathbf{y}}\phi(\cdot, \mathbf{y}; \theta) = \frac{\lambda^{(1)}(\cdot, \mathbf{y}; \theta)}{\lambda(\cdot, \mathbf{y}; \theta)}. \tag{2.13}$$

In practice, this equation is solved numerically, see Section 2.5 and Appendix A.

Having solved (2.13), the covariance and sensitivity matrices for the resulting estimating function

$$e_\phi(\theta) = \sum_{u \in \mathbf{X}} \phi(u, \mathbf{X} \setminus u; \theta) - \int_W \phi(u, \mathbf{X}; \theta)\lambda(u, \mathbf{X}; \theta)\, \mathrm{d}u \tag{2.14}$$

are given by

$$\begin{aligned} S &= \mathrm{E} \int_W \phi(u, \mathbf{X}; \theta)\lambda^{(1)}(u, \mathbf{X}; \theta)^\top \, \mathrm{d}u \\ \Sigma &= S + \mathrm{E} \int_W \int_W \Delta_u\phi(v, \mathbf{X}; \theta)\Delta_v\phi(u, \mathbf{X}; \theta)^\top \lambda(\{u, v\}, \mathbf{X}; \theta)\, \mathrm{d}u\, \mathrm{d}v. \end{aligned}$$

Note that for a truly optimal ϕ, we would have $S = \Sigma$. In the simulation studies in Section 4.1, we investigate for the Strauss model how close S and Σ are for our semi-optimal ϕ.

2.4 A comparison with optimal intensity estimation

In this section we compare our approach with the problem of optimal intensity estimation for spatial point processes investigated and solved by Guan *et al.* (2015). They consider estimating equations of the form

$$e_h(\theta) = \sum_{u \in \mathbf{X}} h(u; \theta) - \int_W h(u; \theta)\lambda(u; \theta)\, \mathrm{d}u \tag{2.15}$$

to estimate a parametric model $\lambda(\cdot; \theta)$ for the intensity function. Using the Campbell theorem, the sufficient condition (2.6) for e_ϕ to be optimal is equivalent to

$$\int_W h(u; \theta)\lambda(u; \theta) \left\{ \phi(u; \theta) - \frac{\lambda^{(1)}(u; \theta)}{\lambda(u; \theta)} + T\phi(u; \theta) \right\} \mathrm{d}u = 0, \tag{2.16}$$

where the operator T acting on $\mathbb{R}^p$ valued functions g is given by

$$Tg(u) = \int_W g(v)\lambda(v; \theta)\{\mathrm{pcf}(v - u) - 1\}\, \mathrm{d}v,$$

where pcf is the so-called pair correlation function. We now compare (2.16) with the condition $\mathrm{E}(A) + \mathrm{E}(B) = 0$ where A and B are given by (2.11)-(2.12).

The terms A and (2.16) are similar where the roles played by the first and second order Papangelou conditional intensities in A correspond to the ones played by the intensity and pair correlation functions in (2.16). However, solving $\mathrm{E}(A) = 0$ is much more complex than solving (2.16). This is mainly due to that the function ϕ is, in the present paper, a function of both $u \in W$ and $\mathbf{y} \in \Omega$: the estimating function (2.15) requires the computation of $\phi(v)$ for $v \in W$ while our estimating function (2.5) requires the evaluation of $\phi(u, \mathbf{x} \setminus u)$ for data points $u \in \mathbf{x}$ as well as the evaluation of $\phi(v, \mathbf{x})$ for $v \in W$, see Appendix A for details on the numerical implementation.

Further, due to the simpler form of (2.15), there is no term like B appearing in (2.16). In the problem we consider, it is not possible to include B and still obtain a condition that is manageable in practice. As mentioned in the previous section, B has been observed to be negligible in certain applications in which case our approach should lead to an estimating equation able to outperform the pseudolikelihood method. As far as we know, our work is the first in this direction.

2.5 Outline of implementation

Let $\mathbf{x} = \{x_1, \ldots, x_n\}$ denote an observation of $\mathbf{X}$. In practice we approximate the integral in (2.9) by numerical quadrature whereby the integral equation (2.13) becomes a matrix equation where for each $\mathbf{y} = \mathbf{x}, \mathbf{x} \setminus x_1, \ldots, \mathbf{x} \setminus x_n$ the unknown quantity is the vector with components $\phi(u_j; \mathbf{y}; \theta)$ where u_j, $j = 1, \ldots, m$, denote the m quadrature points. The detailed description of the implementation which is quite technical and heavy on notation is given in the Appendix.

Depending on the choice of m the solution of the matrix equation involving a sparse $m \times m$ matrix can be computationally quite costly. Since this has to be done for each $\mathbf{y} = \mathbf{x}, \mathbf{x} \setminus x_1, \ldots, \mathbf{x} \setminus x_n$, our method is not recommended for point patterns of large cardinality. In the data examples we provide some examples of computing times. In our applications we use quadrature points located on a regular grid covering W. Thus e.g. for a 50×50 grid, $m = 2500$.

The solution of the matrix equation depends on that the matrix involved is positive definite. For purely repulsive models like the Strauss model and the Strauss hard core model with $\theta_2 < 0$ this was always the case in the data examples and the simulation studies. However in cases of positive interaction where it is possible for the integral operator kernel (2.10) to be negative, the condition of positive definiteness was sometimes violated. This e.g. happened for the multiscale process considered in Section 3.2 and Section 4.2. In such cases we simple returned the pseudolikelihood estimate or restricted the kernel (2.10) to be non-negative, see Section 3.2 and Section 4.2 for more details.

3 Data examples

In this section we present two applications. For the first Spanish towns dataset, we apply a Strauss hard core model. For the second replicated point pattern dataset from neuroscience, we consider a multiscale hard core model.

3.1 Spanish towns dataset

Ripley (1988) and subsequently Illian *et al.* (2008) proposed to model the Spanish towns dataset (see Figure 1) using a Strauss hard core model. We compare results

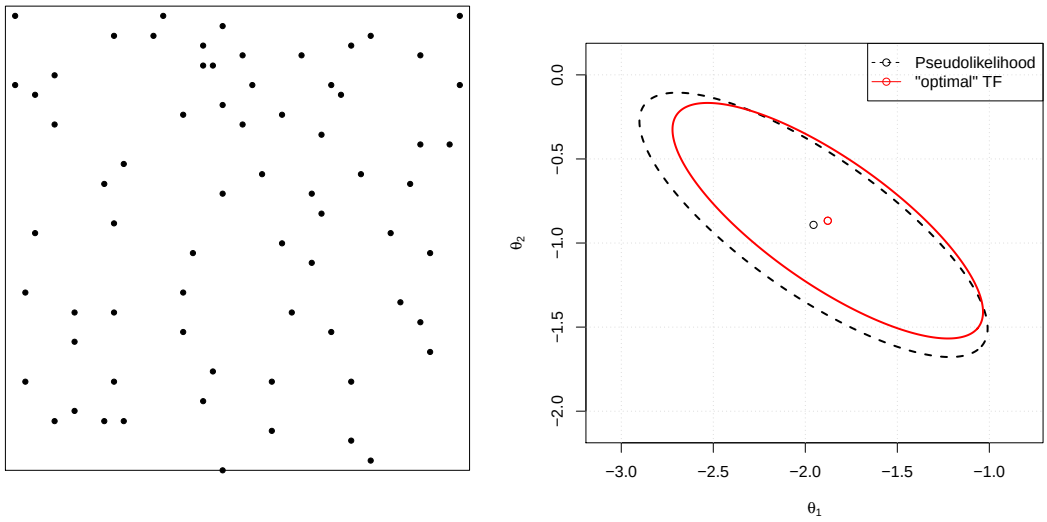

Figure 1: Left: locations of 69 Spanish towns in a 40 miles by 40 miles region. Right: 95% confidence ellipses for the parameters (θ_1, θ_2) for the pseudolikelihood and the semi-optimal Takacs-Fiksel methods.

regarding estimation of θ_1 and θ_2 using respectively the new semi-optimal method and the pseudolikelihood. For the hard core distance and the interaction range we use the values $\widehat{\delta} = 0.83$ and $\widehat{R} = 3.5$ obtained using maximum likelihood by Illian *et al.* (2008, p. 170). For the pseudolikelihood we use the unbiased logistic likelihood implementation introduced in Baddeley *et al.* (2014) with a stratified quadrature point process on a 50×50 grid. The same grid is used for the semi-optimal Takacs-Fiksel method.

Pseudolikelihood and semi-optimal estimates are presented in Table 1. The computing time for obtaining the semi-optimal estimates is 25 seconds on a Lenovo W541 laptop. Standard errors of the pseudolikelihood estimates (respectively the

	θ_1	θ_2
SO	-1.88 (0.12)	-0.87 (0.08)
PL	-1.96 (0.15)	-0.89 (0.10)
Ratio se	0.79	0.79

Table 1: Results for Strauss hard core model applied to the Spanish towns dataset. First and second row: semi-optimal (SO) and pseudolikelihood (PL) estimates with estimated standard errors in parantheses. Last row: ratio of semi-optimal standard errors to pseudolikelihood standard errors.

semi-optimal Takacs-Fiksel estimates) are estimated from 500 simulations of the

model fitted using the pseudolikelihood (respectively the semi-optimal procedure). The standard errors are clearly reduced with the semi-optimal Takacs-Fiksel method. In addition to these results, we compute the Frobenius norm of the estimated covariance matrices for the pseudolikelihood and optimal Takacs-Fiksel estimates (which actually correspond to estimates of the inverse Godambe matrices). We obtained the norm values 0.25 and 0.20 for the pseudolikelihood and the semi-optimal Takacs-Fiksel methods respectively. Based on the asymptotic normality results established by Baddeley *et al.* (2014) and Coeurjolly *et al.* (2012), we construct 95% confidence ellipses for the parameter vector (θ_1, θ_2). The ellipses are depicted in the right plot of Figure 1. The area of the confidence region for the semi-optimal Takacs-Fiksel method is 81% of the one for the pseudolikelihood. In line with the simulation study in Section 4.1, these empirical findings show that more precise parameter estimates can be obtained with the semi-optimal Takacs-Fiksel method compared to pseudolikelihood.

3.2 Application to synaptic vesicles

Synapses are regions in the brain where nerve impulses are transmitted or received. Inside the synapses, neurotransmitters are carried by small membrane-bound compartments called synaptic vesicles. Recently Khanmohammadi *et al.* (2014) studied whether stress affects the spatial distribution of vesicles within the synapse. The data used for the study originated from microscopial images of slices of brains from respectively a group of 6 control rats and a group of 6 stressed rats. The images were annotated to identify the boundaries of the synapses and possible mitochondria in the synapses, the locations of the vesicles, and the extents of the so-called active zones where the vesicles release their contents of neurotransmitters. Figure 2 shows annotations of two images. One synapse was annotated for each rat except for one control rat where two synapses were annotated. Thus in total 7 synapses from the control rats and 6 synapses from the stressed rats were annotated. For each synapse several images corresponding to several slices of the synapse were annotated. We restrict here attention to the middle slice for each synapse. Thus, our data consist of 7 and 6 annotated images for respectively the control and the stressed rats. The side lengths of enclosing rectangles for the synapses range between 396 and 1009 nm with a mean of 663 nm. Further details on the dataset can be found in Khanmohammadi *et al.* (2014).

3.2.1 Point process models for locations of vesicles

For the ith image of type $t = C, S$ (control or stressed) we consider the centers of the vesicles as a realization of a finite spatial point process $\mathbf{X}_{ti}$ with observation window W_{ti} defined by the boundary of the synapse excluding areas occupied by mitochondria. We further assume that the pairs $(W_{ti}, \mathbf{X}_{ti})$ of the observation windows and the spatial point processes for different images are independent, and that pairs $(W_{ti}, \mathbf{X}_{ti})$ of the same type t are identically distributed. Khanmohammadi *et al.* (2014) modelled the locations of the vesicles as an inhomogeneous Strauss hard core process, but noted some evidence of aggregation of vesicles at a larger scale not

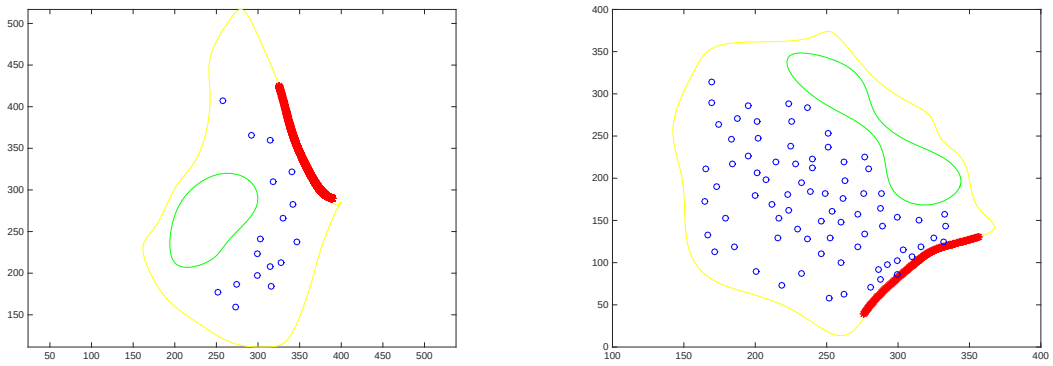

Figure 2: Plots of vesicle locations for a control (left) and a stressed (right) synapse. The active zones are shown by the red curves while the green curves show the boundaries of mitochondria. The yellow curves show the boundaries of the synapses given by their cell membranes.

accommodated by this model. After considering the Strauss hard core model for reference, we therefore extend it to a multiscale model with an additional interaction term. More precisely, for a location u and a configuration $\mathbf{x}$ of vesicle locations in a synapse of type t, the conditional intensity is of the form

$$\lambda_t(u, \mathbf{x}; \theta) = \exp\{\theta_{0t} + \theta_{1t} d(u) + \theta_{2t} s_r(u, \mathbf{x}) + \theta_{3t} s_{r,R}(u, \mathbf{x})\} H_\delta(u, \mathbf{x}), \quad t = C, S \quad (3.1)$$

where $0 \leq \delta < r < R$, $\theta_{0t}, \theta_{1t}, \theta_{2t}, \theta_{3t} \in \mathbb{R}$, $d(u)$ is the distance to the active zone, $s_r(u, \mathbf{x})$ is the number of points in $\mathbf{x}$ with distance to u smaller than r, $s_{r,R}(u, \mathbf{x})$ denotes the number of points in $\mathbf{x}$ with distance to u in the interval $[r, R]$, and the hard core term $H_\delta(u, \mathbf{x})$ is one if all points in $\mathbf{x} \cup u$ are separated by a distance greater than δ and zero otherwise. The inhomogeneous Strauss hard core model is the special case with $\theta_{3t} = 0$. As in Khanmohammadi *et al.* (2014), the hard core distance h is set to 17.5nm corresponding to the average diameter of a vesicle and the interaction distance r is set to 32.5nm. We further choose the value of $R = 107.5$ nm to maximize a profile pseudolikelihood based on the data for all 13 images. We finally scale the distances $d(\cdot)$ by a factor 10^{-3} in order to obtain θ_{lt} estimates of the same order of magnitude.

3.2.2 Inference for replicated point patterns

Let $e^{(ti)}$ denote an estimating function (either the pseudolikelihood score or the semi-optimal) for the tith image and denote by θ_t the vector of parameters to be inferred, $t = C, S$. Then for each type $t = C, S$ we optimally form a pooled estimating function $e^{(t)}$ as the sum of the $e^{(ti)}$'s. Following standard asymptotic arguments for pooled independent estimating functions, the variance of the corresponding parameter estimate is approximated as

$$\mathrm{Var}\left\{\sqrt{n_t}(\hat{\theta}_t - \theta_t)\right\} \approx (S^{t1})^{-1} \mathrm{Var}\left\{e^{(t1)}\right\} (S^{t1})^{-1}$$

(the so-called sandwich estimator, Song, 2007) where n_t is the number of replicates of type t and S^{t1} is the sensitivy matrix associated with $e^{(t1)}$. In practice we replace

	θ_{0C}	θ_{1C}	θ_{2C}
SO	-6.74 (0.21)	-0.68 (0.20)	-2.79 (1.00)
PL	-6.80 (0.21)	-0.66 (0.22)	-2.61 (1.00)
Ratio se	1.01	0.80	1.02
	θ_{0S}	θ_{1S}	θ_{2S}
SO	-5.51 (0.23)	-1.14 (0.47)	-0.61 (0.21)
PL	-5.63 (0.24)	-1.12 (0.49)	-0.45 (0.24)
Ratio se	0.93	0.91	0.78

Table 2: Results for Strauss hard core process. Semi-optimal (SO) and pseudolikelihood (PL) estimates with estimated standard errors in parantheses and ratios of semi-optimal standard errors to pseudolikelihood standard errors. First three rows: control. Last three rows: stressed. Ratios of standard errors were computed before rounding standard errors to two digits.

S^{t1} and $\mathrm{Var}\{e^{(t1)}\}$ by their empirical estimates replacing the unknown θ_t with its estimate. We conduct the pseudolikelihood estimation for the replicated data using the user-friendly `mppm` procedure in the `R` package `spatstat` while using our own code to evaluate the approximate variances of the pseudolikelihood or semi-optimal estimates.

3.2.3 Results for synapse data

Table 2 shows parameter estimates and associated standard errors obtained for the Strauss hard core model with either the pseudolikelihood or the semi-optimal approach. Except for θ_{2S}, the semi-optimal and pseudolikelihood estimates are fairly similar. The qualitative conclusions based on the two types of estimates are identical: negative dependence of conditional intensity on distance and repulsion between vesicles both in the control and the stressed group. The estimated semi-optimal standard errors are smallest for all parameters in the stressed group and θ_{1C} in the control groups. For θ_{0C} and θ_{2C} the estimated semi-optimal and pseudolikelihood standard errors are very similar.

Due to the aforementioned evidence of large scale aggregation we turn to the multiscale model for a more detailed comparison of the control and the stressed group. To avoid problems with negative definiteness in the numerical implementation (see Section 2.5) we restricted θ_{2t} and θ_{3t}, $t = C, S$, to be less or equal to zero inside the kernel (2.10). Parameter estimates and associated standard errors for the multiscale model are shown in Table 3. The qualitative conclusions based on the pseudolikelihood and the semi-optimal estimates coincide. All parameters are significantly different from zero (assuming estimate divided by its standard error is approximately $N(0,1)$). In particular the positive estimates of θ_{3C} and θ_{3S} confirm that there is aggregation at a larger scale. The negative estimates of θ_{1t}, $t = C, S$ indicate that the conditional intensity is decreasing as a function of distance to the active zone while, according to the estimates of θ_{2t}, there appears to be a strong respectively moderate small scale interaction for the control group and the stressed group.

To test the hypotheses: H_l: $\theta_{lS} = \theta_{lC}$, $l = 0, 1, 2, 3$, we consider statistics of the

	θ_{0C}	θ_{1C}	θ_{2C}	θ_{3C}
SO	-8.87 (0.12)	-0.47 (0.11)	-3.40 (0.78)	0.45 (0.02)
PL	-8.71 (0.13)	-0.46 (0.12)	-3.35 (0.80)	0.40 (0.02)
Ratio se	0.94	0.93	0.98	1.01
	θ_{0S}	θ_{1S}	θ_{2S}	θ_{3S}
SO	-7.87 (0.21)	-0.48 (0.26)	-1.17 (0.18)	0.26 (0.02)
PL	-7.84 (0.19)	-0.69 (0.27)	-1.12 (0.18)	0.24 (0.02)
Ratio se	1.12	0.96	0.97	1.07

Table 3: Results for multiscale process. Semi-optimal (SO) and pseudolikelihood (PL) estimates with estimated standard errors in parantheses and ratios of semi-optimal standard errors to pseudolikelihood standard errors. First three rows: control. Last three rows: stressed. Ratios of standard errors were computed before rounding standard errors to two digits.

form $(\hat{\theta}_{lS} - \hat{\theta}_{lC})/\sqrt{\text{se}_{lS}^2 + \text{se}_{lC}^2}$ where se_{lt}^2 denotes the estimated standard error of the estimate $\hat{\theta}_{lt}$ $t = S, C$ and the estimates are obtained either using the semi-optimal approach or pseudolikelihood. Under the hypothesis this statistic is approximately $N(0, 1)$. According to these tests, H_0 and H_2 and H_3 are rejected while H_1 is not irrespective of the estimation method (p-values adjusted for multiple testing using Holm (1979)'s procedure are < 0.001, 0.96, 0.02, < 0.0001 and < 0.001, 0.88, 0.02, < 0.0001 for semi-optimal and pseudolikelihood, respectively). There is thus evidence that the repulsion between vesicles is stronger for the control rats than for the stressed rats which means that the vesicles tend to form more regular patterns for the control rats.

For the control data, the estimated standard errors are smallest with the semi-optimal approach except for θ_{3C}. For the stressed rats the semi-optimal standard errors are smallest for θ_{1S} and θ_{2S} but not for θ_{0S} and θ_{3S}. Overall, a clear pattern is not visible. Note also that the ratios of estimated standard errors should be interpreted with care as they are obviously subject to sampling error. We further compare semi-optimal and pseudolikelihood for the multiscale model in Section 4.2.

The total computing time for fitting the multiscale model to the control and stressed rats datasets is respectively 24 and 18 minutes on a Lenovo W541 laptop. The results shown are obtained using a 80×80 grid. For comparison we also tried a 60×60 grid and got very similar results but with computing time reduced to 6 and 5 minutes. The computing time can be further reduced by running computations for each synapse in parallel.

4 Simulation study

This section investigates by simulation studies the performance of the semi-optimal approach when applied to the models used in the data examples in Section 3.

4.1 Strauss model

To study the performance of our semi-optimal estimating function relative to the pseudolikelihood score, we apply both estimating functions to simulations of a Strauss process (Section 2.1) on the unit square (equivalent to a Strauss hard core model with $\delta = 0$). We use the `spatstat` (Baddeley and Turner, 2005) procedure `rStrauss()` to generate exact simulations of the Strauss process for $\beta = \exp(\theta_1) = 100$ and all combinations of $R = 0.04, 0.08, 0.12$ and $\gamma = \exp(\theta_2) = 0.1, 0.2, 0.4, 0.8$. In the following, we specify parameter settings in terms of the parameters (β, γ) due to their ease of interpretation. We however compare the efficiency of the pseudolikelihood and the semi-optimal estimation methods based on the estimates of θ_1 and θ_2 which are typically closer to being normal than the estimates of β and γ.

The semi-optimal estimating function is implemented using a 50×50 or a 75×75 grid. As in the previous sections, for the pseudolikelihood we use the unbiased logistic likelihood implementation with a stratified quadrature point process. For both estimation methods, R is assumed to be known and equal to the value used to generate the simulations. The biases of the semi-optimal and the pseudolikelihood estimates are very similar. The bias relative to the true parameter estimate is very small (-1 to 1%) for θ_1 but can be substantial for θ_2 (up to 28% in case of $\gamma = \exp(\theta_2) = 0.8$ and $R = 0.04$). However, in all cases the bias is negligible relative to the estimation variance. We therefore focus on root mean square error (RMSE) when comparing the two methods. Due to the small bias relative to estimation variance we would have obtained essentially the same results by replacing RMSE with the standard error of the simulated estimates.

For the parameters θ_1 and θ_2, Table 4 shows for each parameter setting, the RMSE of the pseudolikelihood estimates minus the RMSE of the semi-optimal estimates relative to the RMSE of the pseudolikelihood estimates. For each parameter setting, the RMSEs are estimated from a sample of 1000 parameter estimates obtained from 1000 simulations. We omit simulations where all interpoint distances are larger than R and thus neither the pseudolikelihood nor the semi-optimal estimates of (θ_1, θ_2) exist (if one considered instead (β, γ), an alternative would be to let the estimate of γ be equal to zero when all interpoint distances are greater than R). The reported relative differences in RMSE are subject to Monte Carlo error. Table 4 therefore also shows estimated standard errors for these obtained by applying a bootstrap to each Monte Carlo sample.

Range and grid	Interaction parameter $\gamma = \exp(\theta_2)$ 0.1 θ_1	θ_2	0.2 θ_1	θ_2	0.4 θ_1	θ_2	0.8 θ_1	θ_2
$R = 0.04$								
(50,50)	-1 (0.5)	1 (0.3)	-1 (0.4)	0 (0.2)	-2 (0.3)	0 (0.3)	-2 (0.2)	0 (0.3)
(75,75)	-1 (0.4)	0 (0.2)	-1 (0.3)	0 (0.2)	-1 (0.3)	0 (0.2)	-1 (0.2)	0 (0.2)
$R = 0.08$								
(50,50)	3 (1)	1 (0.6)	0 (0.9)	0 (0.6)	5 (0.8)	2 (0.7)	4 (0.5)	2 (0.7)
(75,75)	2 (0.8)	2 (0.5)	3 (0.9)	2 (0.6)	2 (0.8)	1 (0.7)	1 (0.5)	1 (0.6)
$R = 0.12$								
(50,50)	3 (1.2)	5 (0.8)	4 (1.1)	3 (1)	6 (1.3)	4 (1.3)	5 (1)	4 (1.2)
(75,75)	3 (1.3)	5 (0.9)	7 (1.2)	4 (1)	7 (1.3)	5 (1.2)	7 (1.1)	6 (1.4)

Table 4: RMSE for pseudolikelihood minus RMSE for semi-optimal relative to RMSE for pseudolikelihood (in percent) in case of estimation of θ_1 and θ_2. Grids of 50×50 or 75×75 quadrature points are considered. Numbers between brackets are bootstrap standard errors (in percent).

In case of $R = 0.04$, there is no efficiency improvement by using the semi-optimal estimating function. In fact the semi-optimal approach appears to be sometimes slightly worse than pseudolikelihood, even when taking into account the Monte Carlo error of the estimated relative differences in RMSE. However, for $R = 0.08$ and $R = 0.12$ the semi-optimal approach is always better with decreases up to 5 and 7% in RMSE for semi-optimal relative to RMSE for pseudolikelihood. The results regarding the performance of semi-optimal relative to pseudolikelihood are quite similar for the two choices of grids with slightly more favorable results for semi-optimal in case of the 75×75 grid and $R = 0.12$. For $R = 0.04$ the expected number of points varies from 71 to 92 when γ varies from 0.1 to 0.8. For $R = 0.08$ and $R = 0.12$ the corresponding numbers are 43-75 and 28-61. There does not seem to be a clear dependence on the expected number of simulated points regarding the performance of semi-optimal relative to pseudolikelihood.

For an optimal estimating function and at the true parameter value, the covariance matrix Σ of the estimating function coincides with the sensitivity matrix S. Table 5 shows the estimated relative differences $(S_{ij} - \Sigma_{ij})/\Sigma_{ij}$ in percent for the pseudolikelihood and semi-optimal estimating functions. For neither of the estimating functions, the covariance and sensitivity agree. However, in general the relative deviations are larger for pseudolikelihood than for semi-optimal. To investigate this further, we have computed the Frobenius norms of the matrices with entries $(S_{ij} - \Sigma_{ij})/\Sigma_{ij}$. The results (not shown) indicate that the Frobenius norms for the semi-optimal method are smaller than the corresponding ones for the pseudolikelihood for all cases except $\gamma = 0.8$ and $R = 0.04$.

4.2 Multiscale hard core model

For the multiscale hard core process with conditional intensity

$$\lambda(u, \mathbf{x}; \theta) = \exp\{\theta_0 + \theta_1 d(u) + \theta_2 s_r(u, \mathbf{x}) + \theta_3 s_{r,R}(u, \mathbf{x})\} H_\delta(u, \mathbf{x})$$

	Interaction parameter $\gamma = \exp(\theta_2)$											
Interaction range	0.1			0.2			0.4			0.8		
SO, $R = 0.04$	3	-17	-48	5	-5	-49	2	15	-44	3	-4	-46
0.08	-5	-31	-50	-2	-16	-44	3	-7	-40	1	1	-33
012	-10	-38	-45	-10	-36	-49	-7	-23	-41	-5	-10	-26
PL, $R = 0.04$	41	-4	-46	40	11	-47	27	34	-41	12	4	-43
0.08	87	-4	-46	80	20	-35	71	35	-27	30	27	-20
0.12	119	-3	-37	102	6	-35	87	31	-18	41	32	0

Table 5: Relative difference (in percent) between sensitivity and variance of estimating function, $(S_{ij} - \Sigma_{ij})/\Sigma_{ij}$, $ij = 11, 12, 22$. Upper three rows: semi-optimal (SO). Lower three rows: pseudolikelihood (PL). A grid of 75×75 quadrature points is used.

we consider three settings inspired by the synaptic vesicles data example. The process is simulated on the unit square and we let $d(u) = x$ be the first coordinate of $u = (x, y) \in [0, 1]^2$ and $\theta_1 = -0.5$ to obtain a decreasing trend in the first spatial coordinate. The terms s_r and $s_{r,R}$ and the factor H_δ are defined as below (3.1) with hard core distance $\delta = 0.01$ and interaction ranges $r = 0.08$ and $R = 0.16$. The values of $\gamma_2 = \exp(\theta_2)$ and $\gamma_3 = \exp(\theta_3)$ are $(\gamma_2, \gamma_3) = (0.2, 1)$, $(\gamma_2, \gamma_3) = (0.2, 1.25)$ and $(\gamma_2, \gamma_3) = (0.2, 1.5)$. Note that $\gamma_3 = 1$ corresponds to the null hypothesis of no large scale interaction. The values of $\beta = \exp(\theta_0) = 100, 60, 40$ are adjusted to produce on average 40 points for each of the three parameter settings.

Following the approach in the previous section, Table 6 shows for each parameter setting, the root mean square error (RMSE) of the pseudolikelihood estimates minus the RMSE of the semi-optimal estimates relative to the RMSE of the pseudolikelihood estimates (estimated using 1000 simulations and using a 60×60 grid). As in the previous section we omit cases where neither the semi-optimal nor the pseudolikelihood estimates of $\theta = (\theta_0, \theta_1, \theta_2, \theta_3)$ exist. For the setting with $\gamma_3 = 1.5$ (last two rows of Table 6) we often (24% of the simulations) encountered negative definiteness in the numerical computations. The results in the last row of Table 6 are obtained with θ_2 and θ_3 restricted to be less than or equal to zero inside the kernel (2.10) in which case the negative definiteness only occurred for 2% of the simulations. As mentioned in Section 2.5, we just return the pseudolikelihood estimates in the cases where the semi-optimal approach fails.

For $\gamma_3 = 1$ and $\gamma_3 = 1.25$ the semi-optimal approach performs much better than pseudolikelihood with decreases in relative RMSE of up to 10%. In case of $\gamma_3 = 1.5$ decreases up to 5% are obtained in the last row with the restricted version of the kernel (2.10). With $\gamma_3 = 1.5$ and without restriction (third row), only very moderate decreases are obtained for θ_0, θ_1 and θ_3 while for θ_2, the semi-optimal approach appears to be slightly worse than pseudolikelihood.

5 Discussion

In this paper, we have investigated the scope for outperforming the pseudolikelihood by tuning weight functions for the Takacs-Fiksel estimator. Due to the complicated

$(\beta, \gamma_2, \gamma_3)$	θ_0	θ_1	θ_2	θ_3
(100,0.2,100)				
	5 (1)	6 (1)	3 (1)	10 (1)
(60,0.2,1.25)				
	7 (1)	4 (1)	2 (1)	10 (1)
(40,0.2,1.5)				
	3 (1)	1 (1)	-1 (1)	1 (1)
(40,0.2,1.5)				
	0 (1)	5 (1)	2 (1)	5 (1)

Table 6: RMSE for pseudolikelihood minus RMSE for semi-optimal relative to RMSE for pseudolikelihood (in percent) in case of estimation of $(\theta_0, \theta_1, \theta_2, \theta_3)$. Numbers between brackets are bootstrap standard errors (in percent). In the last row, θ_2 and θ_3 are restricted to be non-positive in the kernel (2.10).

nature of moments for Gibbs point processes, the method is less straightforward than the one proposed by Guan *et al.* (2015) for estimating the intensity function of a spatial point process. Therefore our new Takacs-Fiksel method is not guaranteed to be optimal. It is also computationally more expensive than the approach in Guan *et al.* (2015) because the weight function needs to be evaluated for both the observed point pattern and all patterns obtained by omitting one point at a time.

In the simulation studies we have demonstrated that the new semi-optimal approach can yield better statistical efficiency both for purely repulsive point processes and also certain multiscale models with moderate positive interaction. In presence of stronger positive interactions, the method is, however, susceptible to numerical problems. These numerical problems can, to some extent, be mitigated by introducing restrictions in the kernel (2.10). When comparing the methods, the higher computational complexity of the semi-optimal approach should also be taken into account. Thus, while we have made a significant step towards optimal Takacs-Fiksel estimation there is still room for further improvement.

Acknowledgments

We thank the editor and two referees for detailed and constructive comments that helped to improve the paper. R. Waagepetersen is supported by the Danish Council for Independent Research | Natural Sciences, grant 12-124675, "Mathematical and Statistical Analysis of Spatial Data", and by the "Centre for Stochastic Geometry and Advanced Bioimaging", funded by grant 8721 from the Villum Foundation. J.-F. Coeurjolly is supported by ANR-11-LABX-0025 PERSYVAL-Lab (2011, project OculoNimbus).

References

Baddeley, A. & Turner, R. (2000). Practical maximum pseudolikelihood for spatial point patterns. *Australian and New Zealand Journal of Statistics* **42**, 283–322.

Baddeley, A. & Turner, R. (2005). Spatstat: an R package for analyzing spatial point patterns. *Journal of Statistical Software* **12**, 1–42.

Baddeley, A., Turner, R., Møller, J. & Hazelton, M. (2005). Residual analysis for spatial point processes (with discussion). *Journal of the Royal Statistical Society: Series B (Statistical Methodology)* **67**(5), 617–666.

Baddeley, A., Coeurjolly, J.-F., Rubak, E. & Waagepetersen, R. (2014). Logistic regression for spatial Gibbs point processes. *Biometrika* **101**, 377–392.

Baddeley, A., Rubak, E. & Turner, R. (2015). *Spatial Point Patterns: Methodology and Applications with R*. CRC Press.

Berman, M. & Turner, R. (1992). Approximating point process likelihoods with GLIM. *Applied Statistics* **41**, 31–38.

Besag, J. (1977). Some methods of statistical analysis for spatial data. *Bulletin of the International Statistical Institute* **47**, 77–92.

Billiot, J.-M., Coeurjolly, J.-F. & Drouilhet, R. (2008). Maximum pseudolikelihood estimator for exponential family models of marked Gibbs point processes. *Electronic Journal of Statistics* **2**, 234–264.

Coeurjolly, J.-F. & Rubak, E. (2013). Fast covariance estimation for innovations computed from a spatial Gibbs point process. *Scandinavian Journal of Statistics* **40**(4), 669–684.

Coeurjolly, J.-F., Dereudre, D., Drouilhet, R. & Lavancier, F. (2012). Takacs–Fiksel method for stationary marked Gibbs point processes. *Scandinavian Journal of Statistics* **39**(3), 416–443.

Coeurjolly, J.-F., Møller, J. & Waagepetersen, R. (2015). A tutorial on Palm distributions for spatial point processes. Submitted for publication. Available at arXiv:1512.05871.

Davis, T. (2006). *Direct methods for sparse linear systems*. Part of the SIAM Book Series on the Fundamentals of Algorithms, Philadelphia.

Dereudre, D., Drouilhet, R. & Georgii, H.-O. (2012). Existence of Gibbsian point processes with geometry-dependent interactions. *Probability Theory and Related Fields* **153**(3-4), 643–670.

Diggle, P., Fiksel, T., Grabarnik, P., Ogata, Y., Stoyan, D. & Tanemura, M. (1994). On parameter estimation for pairwise interaction point processes. *International Statistical Review* **62**(1), 99–117.

Fiksel, T. (1984). Estimation of parameterized pair potentials of marked and non-marked Gibbsian point processes. *Elektronische Informationsverarbeitung und Kybernetik* **20**, 270–278.

Georgii, H. O. (1976). Canonical and grand canonical Gibbs states for continuum systems. *Communications in Mathematical Physics* **48**(1), 31–51.

Geyer, C. J. (1999). Likelihood inference for spatial point processes. In: *Stochastic Geometry: Likelihood and Computation* (eds. O. E. Barndorff-Nielsen, W. S. Kendall and M. N. M. van Lieshout), Chapman & Hall/CRC, Boca Raton, Florida, 79–140.

Goulard, M., Särkkä, A. & Grabarnik, P. (1996). Parameter estimation for marked Gibbs point processes through the maximum pseudo-likelihood method. *Scandinavian Journal of Statistics* **23**, 365–379.

Guan, Y., Jalilian, A. & Waagepetersen, R. (2015). Quasi-likelihood for spatial point processes. *Journal of the Royal Statistical Society: Series B (Statistical Methodology)* **77**(3), 677–697.

Hackbusch, W. (1995). *Integral Equations: Theory and Numerical Treatment*. Birkhäuser, Basel, Switzerland.

Heyde, C. (1997). *Quasi-likelihood and its application: a general approach to optimal parameter estimation*. Springer Series in Statistics.

Holm, S. (1979). A simple sequentially rejective multiple test procedure. *Scandinavian Journal of Statistics* **65**, 65–70.

Illian, J., Penttinen, A., Stoyan, H. & Stoyan, D. (2008). *Statistical Analysis and Modelling of Spatial Point Patterns*. Statistics in Practice, Wiley, Chichester.

Jensen, J. L. & Künsch, H. R. (1994). On asymptotic normality of pseudo likelihood estimates for pairwise interaction processes. *Annals of the Institute of Statistical Mathematics* **46**, 475–486.

Jensen, J. L. & Møller, J. (1991). Pseudolikelihood for exponential family models of spatial point processes. *Annals of Applied Probability* **1**, 445–461.

Khanmohammadi, M., Waagepetersen, R., Nava, N., Nyengaard, J. R. & Sporring, J. (2014). Analysing the distribution of synaptic vesicles using a spatial point process model. In: *Proceedings of the 5th ACM Conference on Bioinformatics, Computational Biology, and Health Informatics, BCB '14, Newport Beach, California, USA, September 20-23, 2014*, 73–78.

van Lieshout, M. (2000). *Markov Point Processes and their Applications*. Imperial College Press, London.

Mase, S. (1999). Marked Gibbs processes and asymptotic normality of maximum pseudo-likelihood estimators. *Mathematische Nachrichten* **209**, 151–169.

Møller, J. & Waagepetersen, R. P. (2004). *Statistical Inference and Simulation for Spatial Point Processes*. Chapman and Hall/CRC, Boca Raton.

Nguyen, X. X. & Zessin, H. (1979). Ergodic theorems for spatial processes. *Zeitschrift für Wahrscheinlichkeitstheorie und verwandte Gebiete* **48**, 133–158.

Nyström, E. J. (1930). Über die praktische auflösung von integralgleichungen mit anwendungen auf randwertaufgaben. *Acta Mathematica* **54**(1), 185–204.

Ogata, Y. & Tanemura, M. (1984). Likelihood analysis of spatial point patterns. *Journal of the Royal Statistical Society: Series B (Statistical Methodology)* **46**, 496–518.

Penttinen, A. (1984). *Modelling Interaction in Spatial Point Patterns: Parameter Estimation by the Maximum Likelihood Method*. Number 7 in Jyväskylä Studies in Computer Science, Economics, and Statistics, Univeristy of Jyväskylä.

Ripley, B. D. (1988). *Statistical Inference for Spatial Processes*. Cambridge University Press, Cambridge.

Song, P. X.-K. (2007). *Correlated data analysis: modeling, analytics, and applications*. Springer Series in Statistics, Springer, New York, NY.

Stoyan, D. & Penttinen, A. (2000). Recent applications of point process methods in forestry statistics. *Statistical Science* **15**(1), 61–78.

Takacs, R. (1986). Estimator for the pair-potential of a Gibbsian point process. *Statistics* **17**, 429–433.

Tomppo, E. (1986). Models and methods for analysing spatial patterns of trees. *Communicationes Instituti Forestalis Fenniae* **138**, 1–65.

Waagepetersen, R. & Guan, Y. (2009). Two-step estimation for inhomogeneous spatial point processes. *Journal of the Royal Statistical Society: Series B (Statistical Methodology)* **71**, 685–702.

A Implementation

Let $\mathbf{x} = \{x_1, \ldots, x_n\}$ denote a realization of $\mathbf{X}$. To solve $e_\phi(\theta) = 0$, we use Newton-Raphson iterations starting at the pseudolikelihood estimate with the Hessian matrix estimated by the empirical sensitivity matrix $\hat{S} = \int_W \phi(u, \mathbf{x}; \theta)\lambda^{(1)}(u, \mathbf{x}; \theta)^\top \, \mathrm{d}u$. To evaluate e_ϕ and $\hat{S}$ we need to solve (2.13) with respect to $\phi(\cdot; \mathbf{y}; \theta)$ for all $\mathbf{y} = \mathbf{x}, \mathbf{x} \setminus x_1, \ldots, \mathbf{x} \setminus x_n$.

A.1 Symmetrization

To ease the implementation and in particular the use of Cholesky decompositions, we symmetrize the operator $T_\mathbf{y}$. This is possible if we assume for any $u, v \in W$ and $\mathbf{y} \in \Omega$, the ratio $\lambda(v, \mathbf{y} \cup u; \theta)/\lambda(v, \mathbf{y}; \theta)$ is symmetric in u and v. This assumption is valid for instance for all pairwise interaction point processes. Indeed, the Papangelou

conditional intensity of such processes is given by $\lambda(u, \mathbf{y}; \theta) = e^{\sum_{w \in \mathbf{y}} \psi(\{w,u\};\theta)}$ where ψ is a real valued function, whereby $\lambda(v, \mathbf{y} \cup u; \theta)/\lambda(v, \mathbf{y}; \theta) = e^{\psi(\{v,u\};\theta)}$.

We now multiply each term of (2.13) by $\sqrt{\lambda(\cdot, \mathbf{y}; \theta)}$ and reformulate the problem to solve

$$\widetilde{\phi}(\cdot, \mathbf{y}; \theta) + \widetilde{T}_{\mathbf{y}} \widetilde{\phi}(\cdot, \mathbf{y}; \theta) = \frac{\lambda^{(1)}(\cdot, \mathbf{y}; \theta)}{\sqrt{\lambda(\cdot, \mathbf{y}; \theta)}} \tag{A.1}$$

with respect to the function $\widetilde{\phi}(\cdot, \mathbf{y}; \theta) = \sqrt{\lambda(\cdot, \mathbf{y}; \theta)}\phi(\cdot, \mathbf{y}; \theta)$ where $\widetilde{T}_{\mathbf{y}}$ is the operator with kernel

$$\widetilde{t}(u, v, \mathbf{y}; \theta) = \sqrt{\lambda(u, \mathbf{y}; \theta)\lambda(v, \mathbf{y}; \theta)} \left\{ 1 - \frac{\lambda(v, \mathbf{y} \cup u; \theta)}{\lambda(v, \mathbf{y}; \theta)} \right\}.$$

Once we have obtained the function $\widetilde{\phi}$, we obtain the semi-optimal function ϕ by $\phi(u, \mathbf{y}; \theta) = \widetilde{\phi}(u, \mathbf{y}; \theta)/\sqrt{\lambda(u, \mathbf{y}; \theta)}$.

A.2 Numerical solution using Nyström approximation

The equation (A.1) is solved numerically using the Nyström approximation (Nyström, 1930). We introduce a quadrature scheme with m quadrature points $u_1, \ldots, u_m \in W$ and associated weights w_j, $j = 1, \ldots, m$, and approximate the operator $T_{\mathbf{y}}$ for any $\mathbb{R}^p$ valued function g by

$$T_{\mathbf{y}} g(u) \approx \sum_{j=1}^{m} g(u_j) t(u, u_j, \mathbf{y}; \theta) w_j.$$

Introducing the quadrature approximation in (A.1) and multiplying each term by $\sqrt{w_i}$, we obtain $\sqrt{w_i}\widetilde{\phi}(u_i, \mathbf{y}; \theta)$, $i = 1, \ldots, m$, as solutions of the linear equations

$$\sqrt{w_i}\widetilde{\phi}(u_i, \mathbf{y}; \theta) + \sum_{j=1}^{m} \sqrt{w_i w_j}\widetilde{t}(u_i, u_j, \mathbf{y}; \theta)\sqrt{w_j}\widetilde{\phi}(u_j, \mathbf{y}; \theta) = \sqrt{w_i}\, \frac{\lambda^{(1)}(u_i, \mathbf{y}; \theta)}{\sqrt{\lambda(u_i, \mathbf{y}; \theta)}},$$

for $i = 1, \ldots, m$. These equations can be reformulated as the matrix equation

$$\left\{ \mathbf{I}_m + \widetilde{\mathbf{T}}(\mathbf{y}; \theta) \right\} \sqrt{w}\widetilde{\phi}(\mathbf{y}; \theta) = \ell(\mathbf{y}; \theta) \tag{A.2}$$

where $\mathbf{I}_m$ is the $m \times m$ identity matrix, $\widetilde{\mathbf{T}}(\mathbf{y}; \theta) = \left\{ \sqrt{w_i w_j}\widetilde{t}(u_i, u_j, \mathbf{y}; \theta) \right\}_{ij}$, $i, j = 1, \ldots, m$, $\ell(\mathbf{y}; \theta)$ is the $m \times p$ matrix with rows $\sqrt{w_i}\lambda^{(1)}(u_i, \mathbf{y}; \theta)^\top / \sqrt{\lambda(u_i, \mathbf{y}; \theta)}$, $i = 1, \ldots, m$, and $\sqrt{w}\widetilde{\phi}(\mathbf{y}; \theta)$ is the $m \times p$ matrix with rows $\sqrt{w_i}\widetilde{\phi}(u_i, \mathbf{y}; \theta)^\top$. The symmetric matrix $\widetilde{\mathbf{T}}(\mathbf{y}; \theta)$ is sparse due to the finite range property. Thus, provided that $\mathbf{I}_m + \widetilde{\mathbf{T}}(\mathbf{y}; \theta)$ is positive definite, the matrix equation can be solved with respect to $\sqrt{w}\widetilde{\phi}(\mathbf{y}; \theta)$ using sparse Cholesky factorization (see Davis, 2006, and the `R` package `Matrix`).

Having solved (A.2) with respect to $\sqrt{w}\widetilde{\phi}(\mathbf{y}; \theta)$, and thus obtaining estimates of $\sqrt{w_i}\widetilde{\phi}(u_i, \mathbf{y}; \theta)$, we obtain estimates $\hat{\phi}(u_i, \mathbf{y}; \theta)$ of $\phi(u_i, \mathbf{y}; \theta)$ via the relation

$\hat{\phi}(u_i, \mathbf{y}; \theta) = \widetilde{\phi}(u_i, \mathbf{y}; \theta)/\sqrt{w_i \lambda(u_i, \mathbf{y}; \theta)}$. Letting $\hat{\phi}(\mathbf{y}; \theta)$ be the $m \times p$ matrix with rows $\hat{\phi}(u_j, \mathbf{y}; \theta)^\top$ the Nyström approximation of $\phi(u, \mathbf{y}; \theta)$ for any $u \in W$ is

$$\hat{\phi}(u, \mathbf{y}; \theta) \approx \frac{\lambda^{(1)}(u, \mathbf{y}; \theta)}{\lambda(u, \mathbf{y}; \theta)} - \hat{\phi}(\mathbf{y}; \theta)^\top \{w_j t(u, u_j, \mathbf{y}; \theta)\}_{j=1}^m.$$

In particular, we obtain the approximations $\hat{\phi}(u, \mathbf{x} \setminus u; \theta)$ of $\phi(u, \mathbf{x} \setminus u; \theta)$, $u \in \mathbf{x}$, which are needed to evaluate the first term in (2.14). Finally, the integral term in (2.14) and the empirical sensitivity are approximated by

$$\hat{\phi}(\mathbf{x}; \theta)^\top \{w_j \lambda(u_j, \mathbf{x}; \theta)\}_{j=1}^m \quad \text{and} \quad \hat{\phi}(\mathbf{x}; \theta)^\top w\lambda^{(1)}(\mathbf{x}; \theta)$$

where $w\lambda^{(1)}(\mathbf{x}; \theta)$ is the $m \times p$ matrix with rows $w_j \lambda^{(1)}(u_j, \mathbf{x}; \theta)^\top$.

A.3 Some computational considerations

The matrix $\mathbf{I}_m + \widetilde{\mathbf{T}}(\mathbf{y}; \theta)$ is not guaranteed to be positive definite. In case of purely repulsive point processes (Papangelou conditional intensity always decreasing when neighbouring points are added), all entries in $\widetilde{\mathbf{T}}(\mathbf{y}; \theta)$ are positive and we did not experience negative definite $\mathbf{I}_m + \widetilde{\mathbf{T}}(\mathbf{y}; \theta)$. However, with models allowing for positive interaction, we occasionally experienced negative definiteness in which case a solution for $\phi(\cdot, \mathbf{y}; \theta)$ cannot be obtained. In such case we simply returned the pseudolikelihood estimate.

In case of a quadrature scheme corresponding to a subdivision of W into square cells of sidelength s the computational complexity of one Newton-Raphson update is roughly of the order $(n + 1)m(R/s)^2$. Thus, the semi-optimal approach is less feasible for data with a high number n of points. Thus we would not recommend using the method for datasets with thousands of points while it is presently quite feasible for datasets with a few hundred points.

In case of e.g. the Strauss hard core process we may encounter $\lambda(u_j, \mathbf{y}; \theta) = 0$. In this case, we use the conventions $\lambda^{(1)}(u_j, \mathbf{y}; \theta)/\sqrt{\lambda(u_j, \mathbf{y}; \theta)} = 0$ and $\lambda(u_j, \mathbf{y} \cup u_j; \theta)/\lambda(u_j, \mathbf{y}; \theta) = 0$.